Effects of corrugation shape on frequency band-gaps for longitudinal wave motion in a periodic elastic layer

Vladislav S. Sorokin[a)]
Department of Mechanical Engineering, Technical University of Denmark, Nils Koppels Allé, Building 404, 2800 Kgs. Lyngby, Denmark

(Received 29 September 2015; revised 29 January 2016; accepted 26 March 2016; published online 18 April 2016)

The paper concerns determining frequency band-gaps for longitudinal wave motion in a periodic waveguide. The waveguide may be considered either as an elastic layer with variable thickness or as a rod with variable cross section. As a result, widths and locations of all frequency band-gaps are determined by means of the method of varying amplitudes. For the general symmetric corrugation shape, the width of each odd band-gap is controlled only by one harmonic in the corrugation series with its number being equal to the number of the band-gap. Widths of even band-gaps, however, are influenced by all the harmonics involved in the corrugation series, so that the lower frequency band-gaps can emerge. These are band-gaps located below the frequency corresponding to the lowest harmonic in the corrugation series. For the general non-symmetric corrugation shape, the *m*th band-gap is controlled only by one, the *m*th, harmonic in the corrugation series. The revealed insights into the mechanism of band-gap formation can be used to predict locations and widths of all frequency band-gaps featured by any corrugation shape. These insights are general and can be valid also for other types of wave motion in periodic structures, e.g., transverse or torsional vibration. © *2016 Acoustical Society of America*. [http://dx.doi.org/10.1121/1.4945988]

[LC] Pages: 1898–1908

I. INTRODUCTION

An essential feature of periodic structures is the presence of frequency band-gaps, i.e., frequency ranges in which waves cannot propagate (Brillouin, 1953). Determination of band-gaps and the corresponding attenuation levels is an important practical problem because periodic structures are used everywhere from vibration isolators and mechanical filters to building frames, bridge trusses, railway tracks, and similar. The present paper concerns determining frequency band-gaps for longitudinal wave motion in a periodic straight elastic layer. More specifically the effects of corrugation shape on widths and locations of band-gaps are to be revealed. The waveguide may be considered either as an elastic layer with the variable thickness or as a rod with the variable cross section with the classical Bernoulli-Euler model being employed.

Analysis of plane elastic waves in one-dimensional waveguides is a popular topic, and Shen and Cao (1999), Ruzzene and Bas (2000), Tongele and Chen (2004), and Wu *et al*. (2009) are just a few examples. Usually such analysis is conducted numerically by means of the transfer matrix method or the spectral element method (cf., e.g., Shen and Cao, 1999; Ruzzene and Bas, 2000; Tongele and Chen, 2004; Wu *et al*., 2009). The present paper, however, implies widths and locations of the frequency band-gaps to be determined analytically. In this sense, the paper follows Nayfeh (1974) in which acoustic wave propagation in a periodic duct was studied by the multiple scales method (Nayfeh and Mook, 1979). Bostrom (1983), El-Bahrawy (1994), and Banerjee and Kundu (2006) consider similar problems in elastodynamics. Here, however, another mathematical model of the corrugated elastic layer is used. In Sorokin (2015), longitudinal wave motion in a periodic straight elastic layer was studied and the lowest band-gaps were determined for four specific corrugation shapes, namely, piece-wise constant, piece-wise linear, biquadratic, and pure harmonic corrugations. Thus in the previously published papers within the topic (e.g., Nayfeh, 1974; Bostrom, 1983; El-Bahrawy, 1994; Banerjee and Kundu, 2006; Sorokin, 2015), only some specific corrugation shapes were considered. Consequently, band-gaps were predicted only for these specific corrugation shapes without revealing the essential relationship between the amplitudes of the harmonics involved in the corrugation series and the widths of the frequency band-gaps. The present paper considers corrugation shape of a general form and provides important insights into the mechanism of the band-gaps formation. For example, it reveals the dependencies of the band-gaps widths on the amplitudes of the harmonics involved in the corrugation series enabling one to predict locations and widths of the frequency band-gaps for any corrugation shape of interest. A novel analytical approach, the method of varying amplitudes (Sorokin and Thomsen, 2015a,b), is employed that has a broader applicability range than the classical methods based on Floquet theorem (Brillouin, 1953; Yakubovich and Starzhinskii, 1975) and the asymptotic methods (Nayfeh and Mook, 1979). The method has been proposed in Sorokin and Thomsen (2015a,b); these papers differ from the present one both in terms of the physical problem considered and the results

[a)]Also at the Institute of Problems in Mechanical Engineering RAS, V.O., Bolshoj pr. 61, St. Petersburg, 199178, Russia. Electronic mail: vladsor@mek.dtu.dk

obtained. The problem under study is a model problem; however, it allows one to reveal some important insights into the mechanism of the band-gaps formation that can be present for any periodic structure and any type of wave motion.

II. GOVERNING EQUATIONS

Consider the following equation describing propagation of a plane longitudinal wave in a non-uniform waveguide with the variable property $\tilde{h}(\tilde{x})$:

$$\frac{\partial}{\partial \tilde{x}}\left(\tilde{h}(\tilde{x})\frac{\partial \tilde{u}(\tilde{x},\tilde{t})}{\partial \tilde{x}}\right)-\frac{1}{c^2}\tilde{h}(\tilde{x})\frac{\partial^2 \tilde{u}(\tilde{x},\tilde{t})}{\partial \tilde{t}^2}=0. \tag{1}$$

The waveguide may be viewed as an elastic layer with the variable thickness $\tilde{h}(\tilde{x})$, so that the wave speed c in Eq. (1) is defined by $c=\sqrt{E/(\rho(1-\upsilon^2))}$, here E is the elastic modulus, ρ density, and υ Poisson's ratio of the plate material. Equation (1) also describes axial waves in a non-uniform rod, with the Bernoulli–Euler model being employed. In this case, $c=\sqrt{E/\rho}$, and $\tilde{h}(\tilde{x})$ is the variable cross-sectional area of the rod. For both cases, $\tilde{u}(\tilde{x},\tilde{t})$ is the axial displacement of the layer at the axial coordinate $\tilde{x}$ and time $\tilde{t}$.

Torsional vibrations of straight rods with spatially varying cross-sections are also described by equations similar to Eq. (1). For example, for a rod with a circular cross section, $\tilde{h}(\tilde{x})$ will be the varying polar moment of inertia, and $c=\sqrt{G/\rho}$, where G is the shear modulus. The equation of transverse vibrations of a string with spatially varying mass per unit length and tension also turns to be similar to Eq. (1). Thus the present study covers different types of wave motion in periodic structures, emphasizing generality and importance of the results.

Assuming a solution of the form $\tilde{u}(\tilde{x},\tilde{t})=\tilde{U}(\tilde{x})e^{i\tilde{\omega}\tilde{t}}$, Eq. (1) reduces to the second order ordinary differential equation for the complex amplitude $\tilde{U}(\tilde{x})$

$$\frac{d}{d\tilde{x}}\left(\tilde{h}(\tilde{x})\frac{d\tilde{U}(\tilde{x})}{d\tilde{x}}\right)+\frac{\tilde{\omega}^2}{c^2}\tilde{h}(\tilde{x})\tilde{U}(\tilde{x})=0. \tag{2}$$

The varying property $\tilde{h}(\tilde{x})$ of the waveguide is assumed to be a periodic function of the coordinate $\tilde{x}$ with period $2l$, so that the size of the periodicity cell is $2l$. Consequently, the displacement $\tilde{U}(\tilde{x})$ and the coordinate $\tilde{x}$ are scaled with respect to l, and the new non-dimensional variables are introduced as $x=\tilde{x}/l$, $U(x)=\tilde{U}(x)/l$, giving

$$\frac{d}{dx}\left(h(x)\frac{dU(x)}{dx}\right)+\omega^2 h(x)U(x)=0, \tag{3}$$

where $\omega=\tilde{\omega}l/c$, and $h(x)=\tilde{h}(x)/l$ for the plate and $h(x)=\tilde{h}(x)/l^2$ for the rod. Equation (3) is the non-dimensional equation describing longitudinal wave propagation in the considered non-uniform periodic waveguide. It may be rewritten in the form

$$U''+\omega^2 U+\frac{h'}{h}U'=0, \tag{4}$$

where primes denote derivatives with respect to the non-dimensional coordinate x. As it is seen, Eq. (4) involves modulation of the coefficient at the first derivative, and thus differs considerably from the classical Hill's equation (see e.g., Yakubovich and Starzhinskii, 1975) which was used as the simplest model of a periodic structure in the classical monograph (Brillouin, 1953).

Corrugation shape of the considered periodic waveguide is assumed to be of a general symmetric form defined by

$$h(x)=1-\frac{\varepsilon}{2}[N_1\cos\pi x+N_3\cos 3\pi x+\cdots+N_{2n-1}\cos(2n-1)\pi x]. \tag{5}$$

Note that due to the choice of the dimensionless parameters, the period of $h(x)$ is equal to 2. Expression (5) in particular, covers the important case of the piece-wise constant corrugation shape

$$\begin{aligned} h(x)&=1+\frac{\varepsilon}{2}, \quad \text{for } x\in(-1,-1/2)\cup(1/2,1)\\ h(x)&=1-\frac{\varepsilon}{2}, \quad \text{for } x\in(-1/2,1/2), \end{aligned} \tag{6}$$

and expanding Eq. (6) into trigonometric Fourier series gives

$$h(x)=1-\frac{2\varepsilon}{\pi}\left[\cos\pi x+\cdots-\frac{(-1)^n}{2n-1}\cos(2n-1)\pi x\right]. \tag{7}$$

The piece-wise linear corrugation shape,

$$\begin{aligned} h(x)&=1-\varepsilon(x+1/2), \text{ for } x\in(-1,0),\\ h(x)&=1+\varepsilon(x-1/2), \text{ for } x\in(0,1), \end{aligned} \tag{8}$$

can be also described by the series [Eq. (5)]

$$h(x)=1-\frac{4\varepsilon}{\pi^2}\left[\cos\pi x+\cdots+\frac{1}{(2n-1)^2}\cos(2n-1)\pi x\right]. \tag{9}$$

Expanding the corrugation shape with discontinuity of the second order

$$\begin{aligned} h(x)&=1+\frac{\varepsilon}{2}\left(1-4(x+1)^2\right), \text{ for } x\in(-1,-1/2),\\ h(x)&=1+\frac{\varepsilon}{2}(-1+4x^2), \text{ for } x\in(-1/2,1/2),\\ h(x)&=1+\frac{\varepsilon}{2}\left(1-4(x-1)^2\right), \text{ for } x\in(1/2,1), \end{aligned} \tag{10}$$

into trigonometric Fourier series, one gets

$$h(x)=1-\frac{16\varepsilon}{\pi^3}\left[\cos\pi x+\cdots-\frac{(-1)^n}{(2n-1)^3}\cos(2n-1)\pi x\right]. \tag{11}$$

As an illustration, these corrugation shapes are presented in Fig. 1, with the pure harmonic corrugation shape

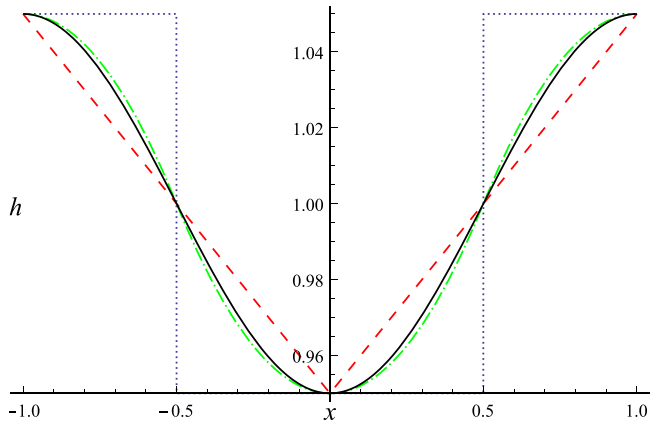

FIG. 1. (Color online) The corrugation shapes for $\varepsilon = 0.1$: piece-wise constant (dotted line), piece-wise linear (dashed line), corrugation with discontinuity of the second order (dashed-dotted line), and pure harmonic corrugation (solid line).

$$h(x) = 1 - \frac{\varepsilon}{2}\cos \pi x, \ \text{for } x \in (-1, 1), \tag{12}$$

also shown for comparison.

The aim of the paper is to reveal essential insights into the mechanism of the band-gap formation, in particular, the relationship between the amplitudes of the harmonics involved in the corrugation series and widths of the frequency band-gaps, and thus the general corrugation form described by expression (5) is considered.

III. SOLUTION BY THE METHOD OF VARYING AMPLITUDES

To determine widths and locations of the frequency band-gaps corresponding to the general corrugation shape [Eq. (5)], the method of varying amplitudes is employed (cf., e.g., Sorokin and Thomsen, 2015a,b). Following the method, a solution of Eq. (3) is sought in the form of series of spatial harmonics with varying amplitudes

$$\begin{aligned} U(x) = \sum_{j=-\infty}^{\infty} b_j(x)\exp(\mathrm{i}j\pi x) = b_0(x) + b_1(x)\exp(\mathrm{i}\pi x) \\ + b_{-1}(x)\exp(-\mathrm{i}\pi x) + b_2(x)\exp(\mathrm{i}2\pi x) \\ + b_{-2}(x)\exp(-\mathrm{i}2\pi x) + \cdots, \end{aligned} \tag{13}$$

where the complex-valued amplitudes $b_j(x)$ are not required to vary slowly in comparison with $\exp(\mathrm{i}j\pi x)$ so that no restrictions on the solution are imposed. We simply reformulate the problem with respect to the new variables $b_j(x)$.

The shift from the original dependent variable $u(x)$ to the new variables $b_j(x)$ implies that additional constraints on these variables should be imposed. With the MVA, the constraints are introduced in the following way: substitute Eq. (13) into the governing Eq. (3) and require the coefficients of the spatial harmonics involved to vanish identically. As the result, one obtains the following infinite set of differential equations for the amplitudes $b_j(x)$:

$$\begin{aligned} & b''_j + \mathrm{i}2j\pi b'_j + \left(\omega^2 - j^2\pi^2\right)b_j \\ & -\frac{\varepsilon}{4}\left(\sum_{k=1}^{\infty} N_{2k-1}[\left(\omega^2 - j(j+1-2k)\pi^2\right)b_{j+1-2k} \right. \\ & + \left(\omega^2 - j(j-1+2k)\pi^2\right)b_{j-1+2k} \\ & + \mathrm{i}\pi\left((2j+1-2k)b'_{j+1-2k} + (2j-1+2k)b'_{j-1+2k}\right) \\ & \left. + b''_{j+1-2k} + b''_{j-1+2k}]\right) = 0, \end{aligned} \tag{14}$$

where j belongs to Z, the set of integer numbers. Solving Eq. (14) is a trivial matter leading to

$$\mathbf{b} = \{b_0 \ b_1 \ b_{-1} \ b_2 \ b_{-2} \ \ldots\}^{\mathrm{T}}, \qquad \mathbf{b}(x) = \mathbf{b}_c \exp(\bar{\kappa}x), \tag{15}$$

where $\bar{\kappa}$ is a root of the characteristic equation of the system [Eq. (14)], and $\mathbf{b}_c$ the associated vector. Thus to determine $\bar{\kappa}$, the infinite determinant of the matrix of the system [Eq. (14)] should be calculated. The diagonal elements of this matrix are given by

$$A[j,j] = (\bar{\kappa} + \mathrm{i}j\pi)^2 + \omega^2, \qquad j \in Z, \tag{16}$$

and all other elements are defined by

$$\begin{aligned} A[j, j+1-2k] = -\frac{\varepsilon}{4}N_{2k-1}\left(\omega^2 + \pi^2\left(\frac{1}{2} - k\right)^2 \right. \\ \left. + \left(\mathrm{i}\pi\left(j + \frac{1}{2} - k\right) + \bar{\kappa}\right)^2\right), \\ j, k \in Z, \ k > 0, \end{aligned} \tag{17}$$

$$\begin{aligned} A[j, j-1+2k] = -\frac{\varepsilon}{4}N_{2k-1}\left(\omega^2 + \pi^2\left(\frac{1}{2} - k\right)^2 \right. \\ \left. + \left(\mathrm{i}\pi\left(j - \frac{1}{2} + k\right) + \bar{\kappa}\right)^2\right), \\ j, k \in Z, \ k > 0. \end{aligned} \tag{18}$$

Note that from expressions (17) and (18), it follows that this matrix is symmetric,

$$A[j, j+1-2k] = A[j+1-2k, j]. \tag{19}$$

Taking into account expression (15), the obtained solution of the Eq. (3) can be written as

$$U(x) = \sum_{j=-\infty}^{\infty} b_{cj}\exp(\mathrm{i}j\pi x)\exp(\bar{\kappa}x). \tag{20}$$

So for the problem considered the MVA gives solution of the same form as direct employing of Floquet theorem (Brillouin, 1953; Yakubovich and Starzhinskii, 1975). From this theorem, it follows that equations with periodic coefficients, in particular, Eq. (3), can have solutions only of the form of Eq. (20). These solutions can be determined by means of the corresponding analytical methods, e.g., the classical Hill's method of infinite determinants (Brillouin, 1953; Yakubovich

and Starzhinskii, 1975; Bolotin, 1964). And the problem reduces to calculating the infinite determinant of the matrix A. Note, however, that the MVA has a broader applicability range than the methods based on Floquet theorem, e.g., it can be employed for nonlinear problems and problems involving multiple excitations with incommensurate frequencies (cf. Sorokin and Thomsen, 2015a,b).

From expression (20), it follows that the solution of the initial governing Eq. (1) takes the form

$$\tilde{u}(x,t) = \tilde{F}(x)\exp(\mathrm{i}(\omega t - \kappa x)), \tag{21}$$

where time t is dimensionless, $t = (c/l)\tilde{t}$, $\kappa = \mathrm{i}\bar{\kappa}$, and $\tilde{F}(x)$ is periodic with respect to x

$$\tilde{F}(x) = lF(x) = l\sum_{j=-\infty}^{\infty} b_{cj}\exp(\mathrm{i}j\pi x). \tag{22}$$

Equation (21) is of the same form as the one obtained by the method of space-harmonics (Mead, 1996). According to Mead (1996) and Brillouin (1953), this solution describes a "compound wave" (Brillouin, 1953) or a "wave package" (Mead, 1996) propagating (or attenuating) in a periodic layer with dimensionless frequency ω. In Brillouin (1953, Sec. 43), κ is named as the wavenumber of the compound wave and in Mead (1996) as the phase constant of the wave motion; real values of κ correspond to propagating waves and complex values to attenuating waves. Note that the notion of the wavenumber as a feature of the compound wave (Brillouin, 1953) differs from the one implied in the asymptotic method of G. Wentzel, H. Kramers, and L. Brillouin (the WKB method) (Pierce, 1970; Nielsen and Sorokin, 2014). The WKB operates with the "local" wavenumber of a wave propagating in a non-uniform structure with this local wavenumber being a function of the spatial coordinate (Pierce, 1970; Nielsen and Sorokin, 2014). However, for studying wave motion in periodic structures, the notion implied in the classical work (Brillouin, 1953) seems to be more convenient.

According to the phase closure principle [Mead, 1996; Nielsen and Sorokin, 2015 (p. 10)] for pure axial waves, frequencies corresponding to boundaries of band-gap regions for linear periodic structures are those where an integer number n of compound half-waves fit exactly into a unit cell of the structure, i.e., these frequencies correspond to the wavenumbers (phase constants)

$$\kappa = \frac{\pi}{2}n, \quad n = \pm 1, \pm 2, \pm 3, ... \tag{23}$$

In the present paper, the relatively weakly modulated waveguide is considered, $\varepsilon \ll 1$. Consequently, the frequencies corresponding to boundaries of the band-gap regions, i.e., to wavenumbers [Eq. (23)], are sought in the form of a series

$$\omega = \omega_0 + \varepsilon\omega_1 + \varepsilon^2\omega_2 + O(\varepsilon^3). \tag{24}$$

This series is then introduced into the algebraic equation

$$\det(A) = 0, \tag{25}$$

along with the values of wavenumbers [Eq. (23)]. Subsequently, ω_0, ω_1, and ω_2 are determined following the classical procedure of expansion in the small parameter ε (Nayfeh and Mook, 1979).

IV. WIDTHS AND LOCATIONS OF ODD BAND-GAPS

First, odd band-gaps are considered which correspond to odd values of n in Eq. (23) (cf. Mead, 1996). Gathering the coefficients of ε^0 in Eq. (25), we obtain the following equation for ω_0, which involves only the diagonal elements of the matrix A because all other elements depend on ε

$$\prod_{m=1}^{\infty}\left(\omega_0^2 - \frac{(2m-1)^2\pi^2}{4}\right)^2 = 0. \tag{26}$$

This equation can be solved explicitly, giving the following positive solutions:

$$\omega_{0,2m-1} = \frac{(2m-1)\pi}{2}, \quad m = 1, 2, 3, ... \tag{27}$$

These values of ω_0 define "seeds" of the band-gaps, i.e., where the band-gaps emerge, with $2m-1$ being the number of the band-gap. For example, the first band-gap emerges at $\omega_{0,1} = \pi/2$, the third at $\omega_{0,3} = 3\pi/2$, etc. Note that seeds of the band-gaps do not depend on the coefficients N_1, N_3, N_5 etc.

Introducing the obtained expression for ω_0 into Eq. (25), one obtains that the coefficient of ε^1 in this equation vanishes. Expressions for ω_1 are then determined from the equation implying the coefficient of ε^2 in Eq. (25) to equal zero

$$\omega_1^2 - \frac{(2m-1)^2\pi^2}{64}N_{2m-1}^2 = 0, \tag{28}$$

which allows for a relatively simple solution of the form

$$\omega_{1,2m-1} = \pm\frac{(2m-1)\pi}{8}N_{2m-1}, \quad m = 1, 2, 3, ..., \tag{29}$$

with $2m-1$ being the number of the band-gap. Combining expression (29) with Eqs. (27) and (24), we obtain that the width of the $2m-1$'th band-gap is determined by

$$\Delta\omega_{2m-1} = \varepsilon\frac{(2m-1)\pi}{4}|N_{2m-1}| + O(\varepsilon^2). \tag{30}$$

Results (27) and (30) indicate that the width and location of the $2m-1$'th band-gap, $m = 1, 2, 3, ...$, for the general corrugation shape [Eq. (5)] are controlled by the $2m-1$'th harmonic in the corrugation series. For example, the width and location of the first band-gap are governed by the first harmonic in the series [Eq. (5)], the third band-gap is controlled by the third harmonic in Eq. (5), etc. Thus it is valid to take into account only the $2m-1$'th harmonic in the series Eq. (5), to determine the width and location of the $2m-1$'th band-gap.

For example, from expression (30), we obtain that the width of the first band-gap for the piece-wise constant corrugation shape Eq. (7) is $\Delta\omega_1 = \varepsilon$, for the piece-wise linear shape Eq. (9) $\Delta\omega_1 = 2\varepsilon/\pi$, for the shape with discontinuity

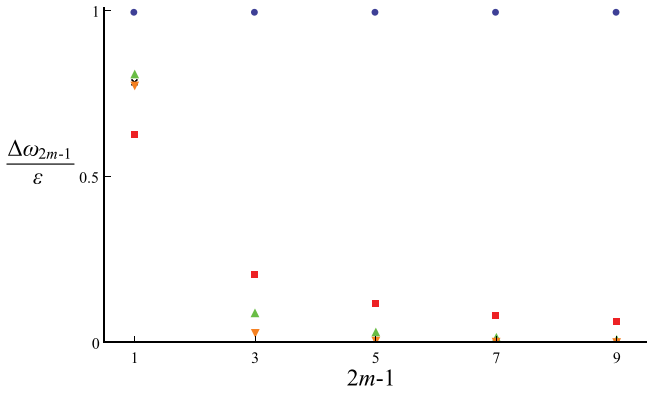

FIG. 2. (Color online) The dependencies of the width $\Delta\omega_{2m-1}/\varepsilon$ of the band-gap on its number $2m-1$ for piece-wise constant corrugation (circles), piece-wise linear corrugation (squares), corrugation with discontinuity of the second order (triangles), corrugation with discontinuity of the third order (inverted triangles), and pure harmonic corrugation (crosses).

of the second order [Eq. (11)] $\Delta\omega_1 = 8\varepsilon/\pi^2$, and for the pure harmonic modulation [Eq. (12)] $\Delta\omega_1 = \pi\varepsilon/4$. These results coincide with those obtained in the paper (Sorokin, 2015), where the first four band-gaps for the piece-wise constant, piece-wise linear, and pure harmonic corrugation shapes were considered. The present paper, however, provides much more general results than those obtained previously because they are applicable for any corrugation shape and concern not only the lowest frequency band-gaps but all of them. For example, general expressions defining widths of all odd band-gaps for the piece-wise constant and the piece-wise linear corrugation shapes, as well as the corrugation shape with discontinuity of the second order, can be derived from expression (30). For the piece-wise constant corrugation shape, we obtain that all odd band-gaps are of the same width

$$\Delta\omega_{2m-1} = \varepsilon, \quad m = 1, 2, 3, ..., \tag{31}$$

for the piece-wise linear shape we get

$$\Delta\omega_{2m-1} = \frac{2}{\pi}\frac{1}{2m-1}\varepsilon, \quad m = 1, 2, 3, ..., \tag{32}$$

so that the width of the band-gap decreases with increasing its number. And for the shape with discontinuity of the second order we obtain

$$\Delta\omega_{2m-1} = \frac{8}{\pi^2}\frac{1}{(2m-1)^2}\varepsilon, \quad m = 1, 2, 3, ..., \tag{33}$$

so that the decrease of the band-gap width with increasing its number is even more pronounced. Thus increasing the order of the discontinuity of the corrugation shape leads to a reduction of the widths of the higher band-gaps. The width of the first band-gap, however, approaches the width of the band-gap for the pure harmonic corrugation. Figure 2 illustrates the obtained dependencies of the band-gap width on its number with the one for the corrugation shape with discontinuity of the third order also shown for comparison

$$h(x) = 1 - \frac{48\varepsilon}{\pi^4}\left[\cos\pi x + \cdots + \frac{1}{(2n-1)^4}\cos(2n-1)\pi x\right]. \tag{34}$$

Also, Fig. 3 presents the dispersion relations obtained by direct solving of Eq. (25) for ω as a function of the wavenumber κ with $\varepsilon = 0.3$; case (a) corresponds to the piece-wise constant corrugation shape, (b) to the piece-wise linear shape, and (c) to the pure harmonic corrugation. As appears from Fig. 3, the dispersion relation is symmetric with respect to the vertical axis and periodic with the wavenumber κ; these results correspond well to those obtained in the classical monograph (Brillouin, 1953).

From expression (30) it also follows that for pure harmonic corrugation shapes described by

$$h(x) = 1 - \frac{\varepsilon}{2}\cos(2n-1)\pi x, \quad n = 1, 2, 3, ..., \tag{35}$$

the widths of the band-gaps increase linearly with increasing n. For example, for the first corrugation shape, $n = 1$, from (30) we get $\Delta\omega_1 = (\pi/4)\varepsilon$, for the second shape, $n = 2$, obtain $\Delta\omega_3 = (3\pi/4)\varepsilon$, and for $n = 3$ get $\Delta\omega_5 = (5\pi/4)\varepsilon$.

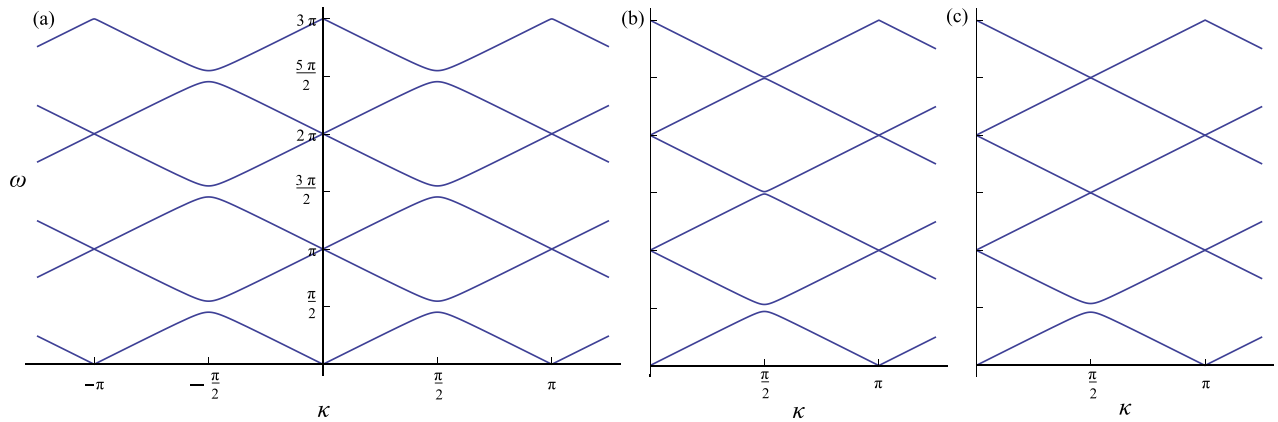

FIG. 3. (Color online) Dispersion relations obtained by direct solving of Eq. (25) for ω as a function of the wavenumber κ, with $\varepsilon = 0.3$; (a) piece-wise constant corrugation shape, (b) piece-wise linear shape, and (c) pure harmonic corrugation.

From expression (30) one finds that if $2m-1$'th harmonic in the series [Eq. (5)] is equal to zero, $N_{2m-1}=0$, then $\omega_{1,2m-1}=0$, and the width of the $2m-1$'th band-gap is of order of ε^2 or smaller. To obtain an explicit expression for the width of the band-gap for this case, we take into account the third term in the series [Eq. (24)]. Introducing this series into Eq. (25), one obtains that for ω_0 defined by expression (27), and $\omega_{1,2m-1}=0$, coefficients of ε^0, ε^1, ε^2, ε^3 in this equation vanish identically. So that ω_2 is to be determined from the equation implying the coefficient of ε^4 in Eq. (25) to be equal to zero. This equation is of the following form:

$$(\omega_2 - f(m,N_1,N_3,N_5,...,N_{2n-1}))^2 = 0, \tag{36}$$

here f is a function of $m,N_1,N_3,N_5,...,N_{2n-1}$, which is rather lengthy, and thus not given here. Equation (36) has two identical roots,

$$\omega_{2,2m-1} = f(m,N_1,N_3,N_5,...,N_{2n-1}). \tag{37}$$

Consequently, from expressions (24) and (37) it follows that

$$\Delta\omega_{2m-1} = O(\varepsilon^3), \quad \text{for } N_{2m-1}=0, \tag{38}$$

i.e., if $2m-1$'th harmonic in the series (5) equals zero, $N_{2m-1}=0$, then the width of the corresponding $2m-1$'th band-gap is of order of ε^3.

Expressions (27), (30), and (38) specify widths and locations of all odd band-gaps for the general symmetric corrugation shape [Eq. (5)]. It is notable that locations of the band-gaps do not depend on the modulation amplitudes, while the width of each band-gap is controlled only by one harmonic in the series [Eq. (5)] with the number of this harmonic being equal to the number of the band-gap. The revealed dependency of the odd band-gaps widths on the modulation amplitudes, apparently, has not yet been discussed in the literature, although it seems to be of considerable practical and theoretical importance because it is valid for any corrugation shape.

V. WIDTHS AND LOCATIONS OF EVEN BAND-GAPS

Now we proceed to determining even band-gaps which correspond to even values of n in expression (23) (cf. Mead, 1996). The first three terms are taken into account in the expansion [Eq. (24)] for ω. Gathering the coefficients of ε^0 in Eq. (25), we obtain the following equation for ω_0:

$$\prod_{m=1}^{\infty}(\omega_0^2 - m^2\pi^2)^2 = 0. \tag{39}$$

The positive solutions for Eq. (39) are

$$\omega_{0,2m} = m\pi, \quad m=1,2,3,.... \tag{40}$$

Thus similarly to the odd band-gaps, locations of even band-gaps do not depend on the modulation amplitudes N_1, N_3, N_5 etc. In Eq. (40), $2m$ is the number of the band-gap, e.g., the second band-gap emerges at $\omega_{0,2}=\pi$, the fourth at $\omega_{0,4}=2\pi$ etc.

The obtained expression (40) for ω_0 leads to vanishing of the coefficient of ε^1 in Eq. (25). The equation for the coefficient of ε^2 in Eq. (25) allows only for the trivial solution

$$\omega_{1,2m}=0, \quad m=1,2,3,..., \tag{41}$$

so that widths of even band-gaps for the general symmetric corrugation shape [Eq. (5)] are of order of ε^2 or smaller.

For ω_0 and ω_1 defined by expressions (40) and (41), respectively, the coefficient of ε^3 in Eq. (25) vanishes. Consequently, ω_2 is determined from the equation implying the coefficient of ε^4 in Eq. (25) to equal zero. This equation is quadratic with respect to ω_2 and rather lengthy, and thus not given here. For $m=1$ and $\omega_{0,2}=\pi$, i.e., for the second band-gap, it allows for the following solutions:

$$\omega_{2,2} = \frac{\pi}{16}\left(\pm\frac{1}{2}N_1^2 \pm \sum_{n=1}^{\infty} N_{2n-1}N_{2n+1} - \sum_{n=1}^{\infty}\frac{(2n-1)^2}{(2n-3)(2n+1)}N_{2n-1}^2\right). \tag{42}$$

Consequently, the width of the second band-gap is determined by

$$\Delta\omega_2 = \frac{\pi}{16}\varepsilon^2\left|N_1^2 + 2\sum_{n=1}^{\infty}N_{2n-1}N_{2n+1}\right| + O(\varepsilon^3). \tag{43}$$

As it is seen from expression (43), the width of the second band-gap depends on *all* the harmonics involved in the series [Eq. (5)]. For example, for the pure harmonic corrugation shape (12) we obtain: $\Delta\omega_2=(\pi/16)\varepsilon^2$. For the piece-wise constant corrugation shape described by the series [Eq. (7)], so that $N_{2n-1}=-(4/\pi)(-1)^n/(2n-1)$, expression (43) immediately gives zero value for the width of the second band-gap

$$\Delta\omega_2 = \frac{1}{\pi}\varepsilon^2\left|1-2\sum_{n=1}^{\infty}\frac{1}{4n^2-1}\right| \to 0. \tag{44}$$

For the piece-wise linear corrugation [Eq. (9)], $N_{2n-1}=(8/\pi^2)\,[1/(2n-1)^2]$, we get

$$\Delta\omega_2 = \frac{4}{\pi^3}\varepsilon^2\left|1+2\sum_{n=1}^{\infty}\frac{1}{(4n^2-1)^2}\right| \to \frac{1}{2\pi}\varepsilon^2. \tag{45}$$

The same results for the second band-gap featured by the piece-wise constant and the piece-wise linear corrugation shapes were obtained in Sorokin (2015). Expression (43), however, enables one to get much more general results that cover any symmetric corrugation shape. For example, for the corrugation shape with discontinuity of the second order [Eq. (11)], $N_{2n-1}=-(32/\pi^3)[(-1)^n/(2n-1)^3]$, from Eq. (43) we get

$$\Delta\omega_2 = \frac{64}{\pi^5}\varepsilon^2\left|1-2\sum_{n=1}^{\infty}\frac{1}{(4n^2-1)^3}\right| \to \frac{6}{\pi^3}\varepsilon^2. \tag{46}$$

As an illustration, Fig. 4 shows the dependencies of the frequencies defining boundaries of the second band-gap on the parameter ε for the pure harmonic, the piece-wise constant and the piece-wise linear corrugation shapes, as well as the corrugation shape with discontinuity of the second order.

It is notable that, in contrast to the odd band-gaps, frequencies defining boundaries of the even band-gaps are not symmetric with respect to the seed of the band-gap ω_0. In particular, as appears from Fig. 4, the second band-gap is shifted to higher frequencies. Expressions (42)–(46) and Fig. 4 indicate that among the presented four corrugation shapes the pure harmonic one features the largest second band-gap.

From expression (43) it also follows that the width of the second band-gap can be non-zero in the case when $N_1 = 0$, so that the corrugation shape

$$h(x) = 1 - \frac{\varepsilon}{2}[N_3 \cos 3\pi x + N_5 \cos 5\pi x + \cdots + N_{2n-1} \cos(2n-1)\pi x] \tag{47}$$

implies a *lower frequency* band-gap, i.e., a band-gap below the frequency $\omega_0 = 3\pi/2$, which is the seed of the lowest band-gap for

$$h(x) = 1 - \frac{\varepsilon}{2} N_3 \sin 3\pi x. \tag{48}$$

This result indicates that additional higher harmonics in the corrugation shape can lead to the lower frequency band-gaps. For example, the corrugation shape

$$h(x) = 1 - \frac{\varepsilon}{2} N_7 \cos 7\pi x \tag{49}$$

features the lowest band-gap at $\omega_0 = 7\pi/2$. However, adding the higher harmonic $-(\varepsilon/2)N_9 \cos 9\pi x$ in expression (49) results in the band-gap emerging at the frequency $\omega_0 = \pi$ which is below $7\pi/2$. These lower frequency band-gaps can be of certain practical and theoretical interest, although they, apparently, have not yet been mentioned in the literature.

For $m = 2$ and $\omega_{0,4} = 2\pi$, i.e., for the fourth band-gap, the following expressions for ω_2 are obtained from the equation implying the coefficient of ε^4 in Eq. (25) to equal zero

$$\omega_{2,4} = \frac{\pi}{8}\left(\pm N_1 N_3 \pm \sum_{n=1}^{\infty} N_{2n-1} N_{2n+3} - \sum_{n=1}^{\infty} \frac{(2n-1)^2}{(2n-5)(2n+3)} N_{2n-1}^2\right). \tag{50}$$

Consequently, the width of the fourth band-gap is determined by

$$\Delta\omega_4 = \frac{\pi}{4}\varepsilon^2 \left| N_1 N_3 + \sum_{n=1}^{\infty} N_{2n-1} N_{2n+3} \right| + O(\varepsilon^3). \tag{51}$$

For example, for the piece-wise constant corrugation shape described by the series [Eq. (7)], expression (51) gives zero value for the width of the fourth band-gap

$$\Delta\omega_4 = \frac{4}{\pi}\varepsilon^2 \left| \frac{1}{3} - \sum_{n=1}^{\infty} \frac{1}{4n^2 + 4n - 3} \right| \to 0. \tag{52}$$

For the piece-wise linear corrugation shape [Eq. (9)] we get

$$\Delta\omega_4 = \frac{16}{\pi^3}\varepsilon^2 \left| \frac{1}{9} + \sum_{n=1}^{\infty} \frac{1}{(4n^2 + 4n - 3)^2} \right| \to \frac{1}{4\pi}\varepsilon^2, \tag{53}$$

which agrees well with the results obtained in Sorokin (2015). The pure harmonic corrugation shape [Eq. (12)] gives the fourth band-gap of the zero width, while the corrugation shape with discontinuity of the second order [Eq. (11)] results in

$$\Delta\omega_4 = \frac{256}{\pi^5}\varepsilon^2 \left| \frac{1}{9} - \sum_{n=1}^{\infty} \frac{1}{(4n^2 + 4n - 3)^3} \right| \to \frac{3}{4\pi^3}\varepsilon^2. \tag{54}$$

As an illustration, Fig. 5 shows the dependencies of the frequencies defining boundaries of the fourth band-gap on the parameter ε for these corrugation shapes.

As appears from Fig. 5, the fourth band-gap is shifted to higher frequencies with respect to $\omega_{0,4} = 2\pi$, and the

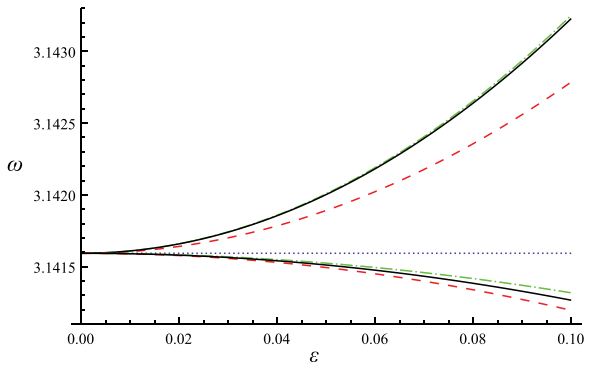

FIG. 4. (Color online) The dependencies of the frequencies defining boundaries of the second band-gap on the parameter ε for piece-wise constant corrugation (dotted line), piece-wise linear corrugation (dashed line), corrugation with discontinuity of the second order (dashed-dotted line), and pure harmonic corrugation (solid line).

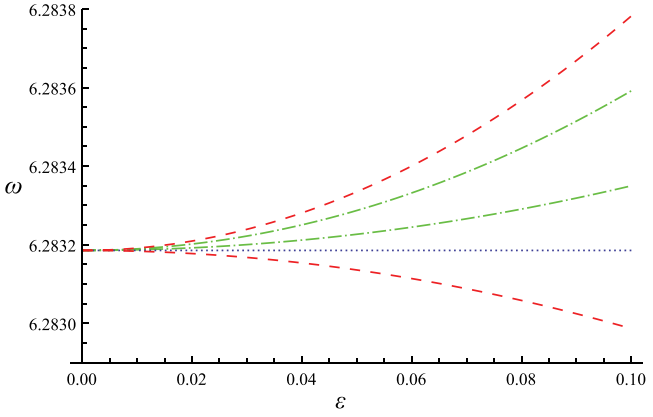

FIG. 5. (Color online) The dependencies of the frequencies defining boundaries of the fourth band-gap on the parameter ε for piece-wise constant corrugation (dotted line), piece-wise linear corrugation (dashed line), and corrugation with discontinuity of the second order (dashed-dotted line).

piece-wise linear corrugation shape features the largest band-gap. Expression (51) also suggests possible emergence of the lower frequency band-gaps. For example, the corrugation shape

$$h(x) = 1 - \frac{\varepsilon}{2} N_5 \cos 5\pi x \tag{55}$$

features the lowest band-gap at $\omega_0 = 5\pi/2$. However, adding the higher harmonic $-(\varepsilon/2)N_9 \cos 9\pi x$ in expression (55) results in the band-gap emerging at the frequency $\omega_0 = 2\pi$ which is below $5\pi/2$.

For $m = 3$ and $\omega_{0,6} = 3\pi$, i.e., for the sixth band-gap, the following expressions for ω_2 are obtained

$$\omega_{2,6} = \frac{3\pi}{16}\left(\pm\frac{1}{2}N_3^2 \pm N_1 N_5 \pm \sum_{n=1}^{\infty} N_{2n-1}N_{2n+5} - \sum_{n=1}^{\infty}\frac{(2n-1)^2}{(2n-7)(2n+5)}N_{2n-1}^2\right). \tag{56}$$

So that the width of the sixth band-gap is determined by

$$\Delta\omega_6 = \frac{3\pi}{16}\varepsilon^2\left|N_3^2 + 2N_1N_5 + 2\sum_{n=1}^{\infty} N_{2n-1}N_{2n+5}\right| + O(\varepsilon^3). \tag{57}$$

And again for the piece-wise constant corrugation shape [Eq. (7)], we get band-gap of the zero width, $\Delta\omega_6 = 0$. For the piece-wise linear shape [Eq. (9)], expression (57) gives

$$\Delta\omega_6 \to \frac{1}{6\pi}\varepsilon^2, \tag{58}$$

while for the corrugation shape with discontinuity of the second order one gets

$$\Delta\omega_6 \to \frac{2}{9\pi^3}\varepsilon^2. \tag{59}$$

For the mth band-gap, expressions for ω_2 take the following form:

$$\omega_{2,2m} = \frac{m\pi}{16}\left(\pm\frac{1}{2}\sum_{n=1}^{m} N_{2n-1}N_{2m-2n+1} \pm \sum_{n=1}^{\infty} N_{2n-1}N_{2n+2m-1} - \sum_{n=1}^{\infty}\frac{(2n-1)^2}{(2n-2m-1)(2n+2m-1)}N_{2n-1}^2\right), \tag{60}$$

and the width of the mth band-gap is determined by

$$\Delta\omega_{2m} = \frac{m\pi}{16}\varepsilon^2\left|\sum_{n=1}^{m} N_{2n-1}N_{2m-2n+1} + 2\sum_{n=1}^{\infty} N_{2n-1}N_{2n+2m-1}\right| + O(\varepsilon^3). \tag{61}$$

Expressions (60)–(61) are general in the sense that they specify widths of all even band-gaps featured by any symmetric corrugation shape; this is in contrast to the previously published results (e.g., Nayfeh, 1974; Bostrom, 1983; El-Bahrawy, 1994; Banerjee and Kundu, 2006; Sorokin, 2015), which correspond to some specific corrugation shapes and predict only the lowest band-gaps.

For the piece-wise constant corrugation shape [Eq. (7)], expression (61) gives zero widths for all even band-gaps

$$\Delta\omega_{2m} = \frac{m}{\pi}\varepsilon^2\left|\sum_{n=1}^{m}\frac{1}{2n-1}\frac{1}{2m-2n+1} - 2\sum_{n=1}^{\infty}\frac{1}{2n-1}\frac{1}{2n+2m-1}\right| \to 0. \tag{62}$$

The piece-wise linear corrugation shape [Eq. (9)] results in

$$\Delta\omega_{2m} = \frac{4m}{\pi^3}\varepsilon^2\left|\sum_{n=1}^{m}\frac{1}{(2n-1)^2}\frac{1}{(2m-2n+1)^2} + 2\sum_{n=1}^{\infty}\frac{1}{(2n-1)^2}\frac{1}{(2n+2m-1)^2}\right| \to \frac{1}{2m\pi}\varepsilon^2, \tag{63}$$

while the corrugation shape with discontinuity of the second order gives

$$\Delta\omega_{2m} \to \frac{6}{m^3\pi^3}\varepsilon^2. \tag{64}$$

Expressions (40) and (61) specify widths and locations of all even band-gaps for the general symmetric corrugation shape [Eq. (5)]. Similarly to the odd band-gaps, locations of even band-gaps do not depend on the modulation amplitudes. However, widths of even band-gaps are influenced by *all* the harmonics involved in the series [Eq. (5)] in the way specified by expression (61). The obtained expressions provide essential insights into the mechanism of the band-gaps formation and enable one to predict widths of all even frequency band-gaps featured by any symmetric corrugation shape.

VI. GENERAL NON-SYMMETRIC CORRUGATION SHAPE

Although the general *symmetric* corrugation shape [Eq. (5)] is of primary interest for applications, e.g., because it covers the important cases of the piece-wise linear and the piece–wise constant corrugations, the case of the general *non-symmetric* corrugation shape is also to be considered

$$h(x) = 1 - \frac{\varepsilon}{2}[N_1 \cos \pi x + N_2 \cos 2\pi x + \cdots + N_n \cos n\pi x]. \tag{65}$$

Employing the MVA and searching the solution in the form [Eq. (13)], we obtain the following infinite set of differential equations for the amplitudes $b_j(x)$:

$$b''_j + \mathrm{i}2j\pi b'_j + (\omega^2 - j^2\pi^2)b_j - \frac{\varepsilon}{4}\left(\sum_{k=1}^{\infty} N_k\left[(\omega^2 - j(j-k)\pi^2)b_{j-k} + (\omega^2 - j(j+k)\pi^2)b_{j+k} + \mathrm{i}\pi((2j-k)b'_{j-k} + (2j+k)b'_{j+k}) + b''_{j-k} + b''_{j+k}\right]\right) = 0. \quad (66)$$

Equation (66) have solutions of the form [Eq. (15)], so that the problem reduces to calculating the infinite determinant of the matrix of the system [Eq. (66)]. The diagonal elements of this matrix are given by expressions (16), and all other elements are defined by

$$A[j,j-k] = -\frac{\varepsilon}{4}N_{|k|}\left(\omega^2 + \frac{\pi^2}{4}k^2 + \left(\mathrm{i}\frac{\pi}{2}(2j-k) + \bar{\kappa}\right)^2\right), \quad j,k \in Z,\ k \neq 0. \quad (67)$$

Following the same procedure as in Sec. IV, we obtain similar expressions for the "seeds" of the band-gaps

$$\omega_{0,m} = \frac{m\pi}{2}, \quad m = 1,2,3,.... \quad (68)$$

Here m is the number of the band-gap. As expected, locations of all band-gaps do not depend on the modulation amplitudes N_1, N_2, N_3 etc.

Expressions for ω_1 are then determined from the equation implying the coefficient of ε^2 in Eq. (25) to equal zero. This equation allows for the following solutions:

$$\omega_{1,m} = \pm\frac{m\pi}{8}N_m, \quad m = 1,2,3,..., \quad (69)$$

here again m is the number of the band-gap. Consequently, for the width of the mth band-gap we get

$$\Delta\omega_m = \varepsilon\frac{m\pi}{4}|N_m| + O(\varepsilon^2). \quad (70)$$

Expressions (68)–(70) are in good agreement with those obtained for the general *symmetric* corrugation shape [Eq. (5)]; for odd band-gaps, they give the same results as obtained in Sec. IV, i.e., Eqs. (27), (29), and (30), and for even band-gaps they reduce to expressions (40) and (41). From relations [Eqs. (68)–(70)], it follows that for the general *non-symmetric* corrugation shape [Eq.(65)], the width and location of the mth band-gap are controlled by the mth harmonic in the corrugation series. For example, the width and location of the first band-gap are governed by the first harmonic in the series (65), the second band-gap is controlled by the second harmonic in [Eq.(65)] etc. Thus it is valid to take into account only one, mth, harmonic in the series (65), to determine the width of the mth band-gap to the leading order. These results also spread much beyond those previously published, e.g., in Sorokin (2015).

It should be also noted that the corrugation shape involving only even harmonics

$$h(x) = 1 - \frac{\varepsilon}{2}[N_2\cos 2\pi x + \cdots + N_{2n}\cos 2n\pi x], \quad (71)$$

can be reduced to the considered general non-symmetric corrugation shape [Eq. (65)] by introducing the new spatial coordinate $x_1 = 2x$,

$$h(x_1) = 1 - \frac{\varepsilon}{2}[N_2\cos \pi x_1 + \cdots + N_{2n}\cos n\pi x_1]. \quad (72)$$

Equation (3) then transforms into

$$\frac{d}{dx_1}\left(h(x_1)\frac{dU(x_1)}{dx_1}\right) + \bar{\omega}^2 h(x_1)U(x_1) = 0, \quad (73)$$

here $\bar{\omega} = \omega/2$. So that from expression (68) for the "seeds" of the band-gaps corresponding to the corrugation shape (71) we get

$$\omega_{0,m} = 2\bar{\omega}_{0,m} = m\pi, \quad m = 1,2,3,.... \quad (74)$$

Here m is the number of the band-gap. From relation [Eq. (69)] for $\omega_{1,m}$ we then get

$$\omega_{1,m} = 2\bar{\omega}_{1,m} = \pm\frac{m\pi}{4}N_{2m}, \quad m = 1,2,3,..., \quad (75)$$

so that the width of the mth band-gap is determined by

$$\Delta\omega_m = 2\Delta\bar{\omega}_m = \varepsilon\frac{m\pi}{2}|N_{2m}| + O(\varepsilon^2). \quad (76)$$

Results [Eqs. (74)–(76)] indicate that the corrugation shape [Eq. (71)] involving only even harmonics cannot feature odd band-gaps, i.e., band-gaps corresponding to odd harmonics in the corrugation series. This is in contrast to the general *symmetric* corrugation shape [Eq. (5)] involving only odd harmonics but featuring even band-gaps. This qualitative difference can be explained by the fact these corrugation shapes have different periodicities: period of Eq. (5) is equal to 2, while period of Eq. (71) is equal to 1.

VII. VALIDATION OF THE RESULTS

As appears form the theoretical analysis described in the preceding text, the only approximation employed is concerned with the representation of the frequency ω in the form of series [Eq. (24)] and subsequent solving of the algebraic equation [Eq. (25)] using the classical procedure of expansion in the small parameter ε. This procedure has been given strict mathematical justification, cf., e.g., Nayfeh and Mook (1979) with both the applicability range and the solution accuracy being explicitly specified. Thus the obtained expressions for the frequency band-gaps are valid and accurate to the given order of ε.

However, to further validate the results obtained in the present paper, a series of numerical experiments was conducted. Employing the non-dimensional variables x and t, and introducing $u(x,t) = \tilde{u}(x,t)/l$, we first rewrite the initial governing equation [Eq. (1)] in the non-dimensional form

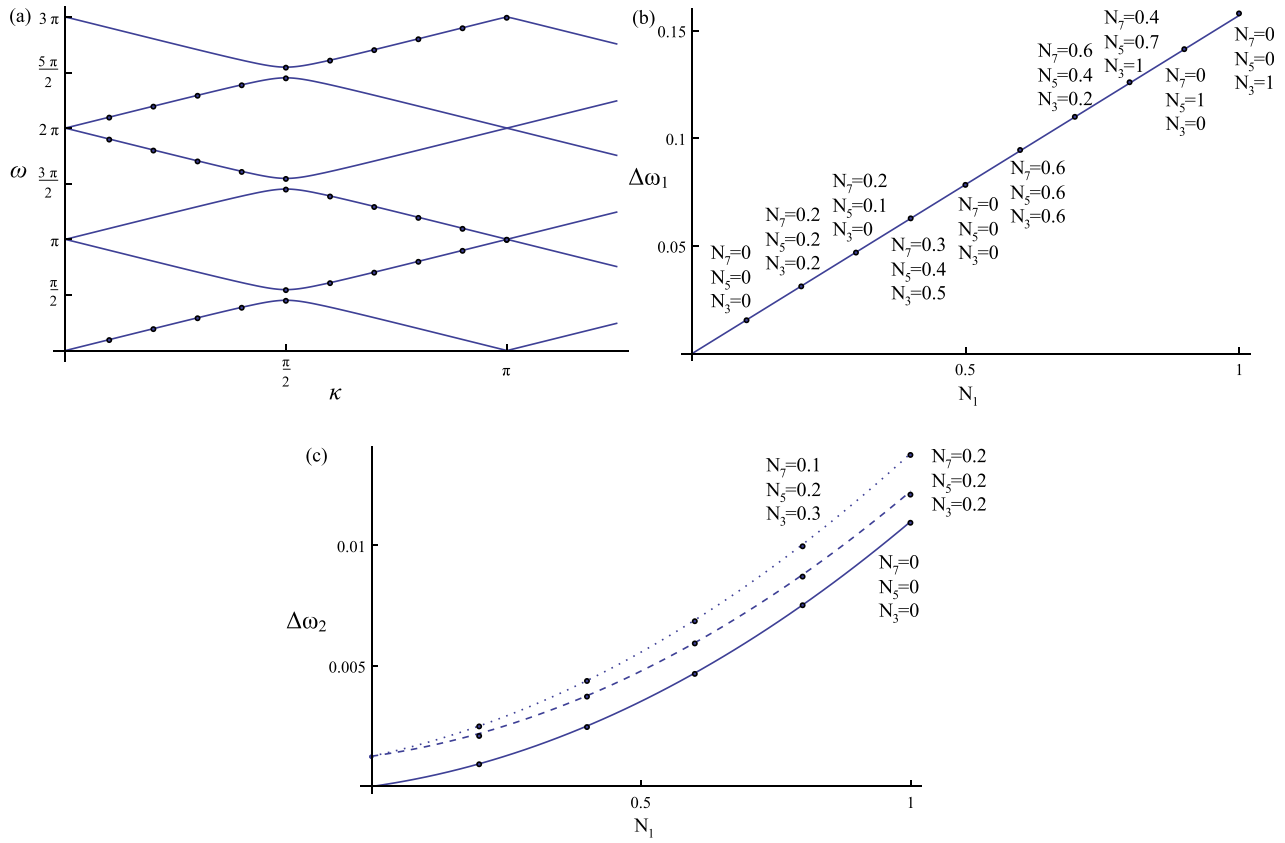

FIG. 6. (Color online) Validation by numerical experiments; lines represent analytical results and filled circles numerical data: (a) the dispersion relation for the piece-wise constant corrugation shape for $\varepsilon = 0.3$; (b) the dependency of the width of the first frequency band-gap $\Delta\omega_1$ on the amplitude N_1 for $\varepsilon = 0.2$ and various values of the corrugation amplitudes N_3, N_5, and N_7 specified near the filled circles; (c) the dependency of the width of the second frequency band-gap $\Delta\omega_2$ on the amplitude N_1 for $\varepsilon = 0.2$; solid line corresponds to $N_3 = N_5 = N_7 = 0$, dashed line to $N_3 = N_5 = N_7 = 0.2$, and dotted line to $N_3 = 0.3$, $N_5 = 0.2$, and $N_7 = 0.1$.

$$\frac{\partial}{\partial x}\left(h(x)\frac{\partial u(x,t)}{\partial x}\right) - h(x)\frac{\partial^2 u(x,t)}{\partial t^2} = 0. \tag{77}$$

This equation is then numerically integrated directly using WOLFRAM MATHEMATICA 7.0 (NDSolve), with periodic boundary conditions and the following initial conditions imposed:

$$u(x,0) = F(x)\exp(-\mathrm{i}\kappa x) = \sum_{j=-\infty}^{\infty} b_{cj}\exp(\mathrm{i}j\pi x)\exp(-\mathrm{i}\kappa x)$$

$$\frac{\partial u}{\partial t}(x,0) = 0. \tag{78}$$

These initial conditions correspond to the obtained analytical solution [Eqs. (21) and (22)]. Consequently, in accordance with the theoretical predictions, at such initial conditions the considered periodic structure should oscillate with the frequency ω. This allows for validating the obtained dispersion relations between frequency ω and wavenumber κ and the expressions for the frequency band-gaps as well as the obtained solution [Eq. (21)] itself.

Typical results of the numerical experiments are shown in Fig. 6, where lines represent analytical results and filled circles numerical data for various values of the parameters. Figure 6(a) shows the dispersion relation for the piece-wise constant corrugation shape for $\varepsilon = 0.3$. As it appears there is no discrepancy between numerical and analytical values of the frequency ω. Similar results were obtained for the other corrugation shapes. Figure 6(b) shows the dependency of the width of the first frequency band-gap $\Delta\omega_1$ on the amplitude N_1 for $\varepsilon = 0.2$; here numerical data correspond to various values of the corrugation amplitudes N_3, N_5, and N_7, which are specified near the filled circles. As appears the width of the band-gap does not depend on the amplitudes N_3, N_5, and N_7, as it was predicted theoretically. Similar results were obtained also for the higher odd frequency band-gaps, and thus the insights revealed in Sec. IV were validated numerically. Figure 6(c) shows the dependency of the width of the second frequency band-gap $\Delta\omega_2$ on the amplitude N_1 for $\varepsilon = 0.2$ and various values of the other corrugation amplitudes N_3, N_5, and N_7; solid line corresponds to $N_3 = N_5 = N_7 = 0$, dashed line to $N_3 = N_5 = N_7 = 0.2$, and dotted line to $N_3 = 0.3$, $N_5 = 0.2$, and $N_7 = 0.1$. As appears there is a good agreement between numerical and analytical results, which is present also for the higher even frequency band-gaps. Thus the insights into the band-gap formation revealed in Sec. V were also validated numerically.

VIII. CONCLUSIONS

The paper concerns determining widths and locations of the frequency band-gaps for longitudinal wave motion in a periodic waveguide. The considered waveguide models both

an elastic layer with a variable periodic thickness and a rod with a variable periodic cross section, with the classical Bernoulli–Euler approximation being employed. As the result, general expressions for the widths and locations of all frequency band-gaps that are featured by the general corrugation shape are determined by means of the method of varying amplitudes. In particular, the dependency of the band-gaps widths on the amplitudes of the harmonics involved in the corrugation series is revealed; it is also shown that locations of the band-gaps do not depend on these amplitudes. The obtained results can be used to predict locations and widths of all frequency band-gaps for any corrugation shape of interest and thus are of certain practical and theoretical importance.

For the general symmetric corrugation shape, the width of each odd band-gap is controlled only by one harmonic in the corrugation series with the number of this harmonic being equal to the number of the band-gap. Widths of even band-gaps, however, are influenced by all the harmonics involved in the corrugation series. The emergence of the lower frequency band-gaps is revealed. Such band-gaps, apparently, have not yet been mentioned in the literature, although they seem to be of certain practical and theoretical interest because they are located below the frequency corresponding to the lowest harmonic in the corrugation series.

For the general non-symmetric corrugation shape, the width and location of the *m*th band-gap are controlled by one, the *m*th, harmonic in the corrugation series. It is shown therefore that the method of varying amplitudes is a simple and effective tool to determine all frequency band-gaps featured by a periodic structure, without limitations on the shape or size of the modulation. The insights into the mechanism of the band-gaps formation revealed in the paper, in particular, the relationship between the amplitudes of the harmonics involved in the corrugation series and the widths of the frequency band-gaps, are general in the sense that they can be present also for other types of wave motion in periodic structures, e.g., transverse or torsional vibration.

ACKNOWLEDGMENTS

The author is grateful to Professor S.V. Sorokin for specifying the research subject and valuable comments to the paper. The work was carried out with financial support from the Danish Council for Independent Research and FP7 Marie Curie Actions–COFUND: DFF– 1337-00026.

Banerjee, S., and Kundu, T. (**2006**). "Symmetric and anti-symmetric Rayleigh-Lamb modes in sinusoidally corrugated waveguides: An analytical approach," Int. J. Solids. Struct. **43**, 6551–6567.

Bolotin, V. V. (**1964**). *The Dynamic Stability of Elastic Systems* (Holden-Day, San Francisco), 451 pp.

Bostrom, A. (**1983**). "Acoustic waves in a cylindrical duct with periodically varying cross section," Wave Motion **5**, 59–67.

Brillouin, L. (**1953**). *Wave Propagation in Periodic Structures*, 2nd ed. (Dover Publications, New York), 255 pp.

El-Bahrawy, A. (**1994**). "Stop-bands and pass-bands for symmetrical Rayleigh-Lamb modes in a plate with corrugated surfaces," J. Sound. Vib. **170**(2), 145–160.

Mead, D. J. (**1996**). "Wave propagation in continuous periodic structures: Research contributions from Southampton, 1964-1995," J. Sound. Vib. **190**(3), 495–524.

Nayfeh, A. H. (**1974**). "Sound waves in two-dimensional ducts with sinusoidal walls," J. Acoust. Soc. Am. **56**(3), 768–770.

Nayfeh, A. H., and Mook, D. T. (**1979**). *Nonlinear Oscillations* (Wiley-Interscience, New York), 704 pp.

Nielsen, R. B., and Sorokin, S. V. (**2014**). "The WKB approximation for analysis of wave propagation in curved rods of slowly varying diameter," Proc. R. Soc. A **470**, 20130718.

Nielsen, R. B., and Sorokin, S. V. (**2015**). "Periodicity effects of axial waves in elastic compound rods," J. Sound. Vib. **353**, 135–149.

Pierce, A. D. (**1970**). "Physical interpretation of the WKB or Eikonal approximation for waves and vibrations in inhomogeneous beams and plates," J. Acoust. Soc. Am. **48**(1), 275–284.

Ruzzene, M., and Bas, A. (**2000**). "Attenuation and localization of wave propagation in periodic rods using shape memory alloys," Smart. Mater. Struct. **9**, 805–811.

Shen, M., and Cao, W. (**1999**). "Acoustic band-gap engineering using finite-size layered structures of multiple periodicity," Appl. Phys. Lett. **75**, 3713–3715.

Sorokin, S. V. (**2015**). "On propagation of plane symmetric waves in a periodically corrugated straight elastic layer," J. Sound. Vib. **349**, 348–360.

Sorokin, V. S., and Thomsen, J. J. (**2015a**). "Vibration suppression for strings with distributed loading using spatial cross-section modulation," J. Sound. Vib. **335**, 66–77.

Sorokin, V. S., and Thomsen, J. J. (**2015b**). "Eigenfrequencies and eigenmodes of a beam with periodically continuously varying spatial properties," J. Sound. Vib. **347**, 14–26.

Tongele, T. N., and Chen, T. (**2004**). "Control of longitudinal wave propagation in conical periodic structures," J. Vib. Control. **10**, 1795–1811.

Wu, M.-L., Wu, L.-Y., Yang, W.-P., and Chen, L.-W. (**2009**). "Elastic wave band-gaps of one-dimensional phononic crystals with functionally graded materials," Smart. Mater. Struct. **18**, 115013.

Yakubovich, V. A., and Starzhinskii, V. M. (**1975**). *Linear Differential Equations with Periodic Coefficients* (Wiley and Sons, New York), 839 pp.